Cell PRESS
Open ACCESS
Cell Reports
Report

Nonlinear Decoding and Asymmetric Representation of Neuronal Input Information by CaMKIIα and Calcineurin

Hajime Fujii,[1,3] Masatoshi Inoue,[1] Hiroyuki Okuno,[1,3] Yoshikazu Sano,[2] Sayaka Takemoto-Kimura,[1,4] Kazuo Kitamura,[2,4] Masanobu Kano,[2] and Haruhiko Bito[1,3,*]
[1]Department of Neurochemistry
[2]Department of Neurophysiology
Graduate School of Medicine, The University of Tokyo, 7-3-1 Hongo, Bunkyo-ku, Tokyo 113-0033, Japan
[3]CREST-JST, Chiyoda-ku, Tokyo 102-0076, Japan
[4]PRESTO-JST, Kawaguchi, Saitama 332-0012, Japan
*Correspondence: hbito@m.u-tokyo.ac.jp
http://dx.doi.org/10.1016/j.celrep.2013.03.033

SUMMARY

How information encoded in glutamate release rates at individual synapses is converted into biochemical activation patterns of postsynaptic enzymes remains unexplored. To address this, we developed a dual fluorescence resonance energy transfer (FRET) imaging platform and recorded CaMKIIα and calcineurin activities in hippocampal neurons while varying glutamate uncaging frequencies. With little spine morphological change, 5 Hz spine glutamate uncaging strongly stimulated calcineurin, but not CaMKIIα. In contrast, 20 Hz spine glutamate uncaging, which induced spine growth, activated both CaMKIIα and calcineurin with distinct spatiotemporal kinetics. Higher temporal resolution recording in the soma revealed that CaMKIIα activity summed supralinearly and sensed both higher frequency and input number, thus acting as an input frequency/number decoder. In contrast, calcineurin activity summated sublinearly with increasing input number and showed little frequency dependence, thus functioning as an input number counter. These results provide evidence that CaMKIIα and calcineurin are fine-tuned to unique bandwidths and compute input variables in an asymmetric manner.

INTRODUCTION

The nervous system adapts to a fluctuating environment through the activity-dependent modulation of neuronal properties such as synaptic plasticity (Bliss and Collingridge, 1993; Bito, 1998; Bito and Takemoto-Kimura, 2003; Malenka and Bear, 2004). The direction and extent of such sustainable modulation is determined by the stimulus parameters (Dudek and Bear, 1992), suggesting that the biochemical machineries that operate at synapses can readily compute the input information (Lisman, 1989; De Koninck and Schulman, 1998; Bhalla, 2002; Wyatt et al., 2012). Ca^{2+}- and calmodulin-dependent kinase II (CaMKII) and calcineurin (also known as protein phosphatase 2B) appear to play key roles in these processes (Malinow et al., 1988; Klee, 1991; Silva et al., 1992; Mulkey et al., 1994; Zhuo et al., 1999; Malleret et al., 2001; Zeng et al., 2001; Hudmon and Schulman, 2002; Colbran, 2004; Coultrap and Bayer, 2012).

Synaptic plasticity is associated with changes in the morphology of dendritic spines that can be induced at the single-synapse level (Matsuzaki et al., 2004). Pharmacological data have implicated the involvement of CaMKII and calcineurin in such changes in spine morphology (Matsuzaki et al., 2004; Zhou et al., 2004). Fluorescence resonance energy transfer (FRET) imaging combined with single-spine glutamate uncaging has proven to be powerful in determining the biochemical correlates of spine morphological plasticity induction (Lee et al., 2009).

However, several important theoretical postulates underlying the role of CaMKII and calcineurin during synaptic plasticity—e.g., that CaMKII in spines functions as a high-frequency input detector or that calcineurin is uniquely activated by low-frequency stimulation—remain untested in living neurons. In particular, although dendritic glutamate uncaging has been successfully applied for the study of the contribution of temporal input sequences (Branco et al., 2010), glutamate uncaging frequency was not systematically varied in previous studies. Therefore, evidence is lacking as to whether distinct sets of incoming glutamate stimulation parameters can be transformed into differential spatiotemporal activation patterns of the Ca^{2+}-sensitive biochemical effectors. Furthermore, although some models proposed a critical role of the calcineurin-inhibitor-1-protein phosphatase-1 pathway in regulating CaMKII activity during plasticity (Lisman, 1989; Klee, 1991; Bhalla, 2002), these ideas were not directly examined in hippocampal neurons.

To address these issues, we have developed an integrated all-optical platform, designated dFOMA (dual FRET with optical manipulation) imaging, and demonstrate that CaMKIIα and calcineurin independently, rather than oppositely, sense synaptic inputs in an asymmetric manner.

RESULTS

Interrogating the Frequency-Dependent Responses of Dendritic Spines in Cultured Hippocampal Neurons with dFOMA Imaging

As the first step to investigate the relationship between glutamate stimulus patterns (frequency and number) and the activation of spine enzymes in situ, we set out to develop a robust model system in which single synapses are manipulated to discriminate incoming glutamate parameters and accordingly trigger the induction of spine structural plasticity. We applied single spines of rat cultured hippocampal neurons with two alternative frequency protocols for local glutamate uncaging—5 Hz glutamate uncaging (5Hz-GU, 100 pulses of photostimulation at 5 Hz) or 20 Hz glutamate uncaging (20Hz-GU, 100 pulses of photostimulation at 20 Hz)—in the absence of extracellular Mg^{2+} (in order to induce Ca^{2+} influx via NMDA receptors) and monitored spine morphology with mCherry (Shaner et al., 2004) (Figures 1A and S1A). We found that the volume of stimulated spines significantly increased in response to 20Hz-GU but did not change after 5Hz-GU (Figures 1B and S1B). Nonstimulated spines in the same field of view did not manifest any change in morphology (Figure S1C), confirming that the stimulation was indeed highly local. Photostimulation had no significant effect on electrophysiological parameters, such as resting membrane potential, input resistance or miniature EPSC frequencies or amplitudes (Figures S1D–S1I). Thus, it is possible to experimentally manipulate individual spines for the discrimination of the temporal sequence of glutamatergic inputs and to translate this information into induction of morphological plasticity.

How can dendritic spines discriminate 20Hz-GU from 5Hz-GU? Are CaMKIIα and calcineurin able to perform such information processing (Figure 1C)? To address this issue directly, we developed the dFOMA imaging platform, which integrates three distinct optical strategies: FRET-based measurement of enzymatic activity, dual FRET imaging to monitor two independent signals, and optical manipulation by UV-light-induced uncaging of 4-methoxy-7-nitroindolinyl-caged L-glutamate (MNI-glutamate) (Figures 1D and S1J–S1L; see Extended Experimental Procedures). We developed more powerful FRET probes to monitor CaMKIIα and calcineurin activities on the basis of the latest CaMKII holoenzyme structure studies (Gaertner et al., 2004; Chao et al., 2011). Unlike with Camui-type probes (Takao et al., 2005; Lee et al., 2009), to optimize the donor-acceptor proximity during resting state, we incorporated the donor and acceptor fluorescent proteins into the NH_2 terminal domain and an internal variable domain of CaMKIIα, given that both of these regions resided at the external surface of the dodecameric holoenzyme (Figure S1M; see Extended Experimental Procedures) (Gaertner et al., 2004; Chao et al., 2011). The resulting probes were designated K2α for the cyan fluorescent protein (CFP)-yellow fluorescent protein (YFP) version, RS-K2α for the mCherry-Sapphire version, and RY-K2α for the mCherry-YFP version (Nagai et al., 2002; Zapata-Hommer and Griesbeck, 2003; Shaner et al., 2004) (Figures 1D and S1M–S1O). Using in vitro fluorometry, we found that the FRET signal of K2α can quantitatively report three features of CaMKIIα activity: activation by CaM binding, autonomy by autophosphorylation of Thr286, and inactivation by autophosphorylation of Thr305 (Figures S1P–S1T, see Extended Experimental Procedures for details and discussion for K2α). On the basis of an all-optical Lineweaver-Burk plot with FRET-based measures, we found a competitive inhibition mechanism for a CaMK inhibitor, KN-93, with an apparent K_i of 1.24 ± 0.01 μM (Figure S1Q), in perfect keeping with a published value previously determined by ^{32}P incorporation into a substrate peptide (Sumi et al., 1991). Other basic biochemical properties of CaMKIIα were also retained in K2α, such as kinase activity (Figure S1R), Ca^{2+}-dependent binding of CaM (data not shown), and multimerization (data not shown).

On the basis of previous structural studies (Griffith et al., 1995; Kissinger et al., 1995), a calcineurin FRET probe (RY-CaN) for monitoring activation-associated conformational changes was constructed by tagging fluorescent proteins to the NH_2 and COOH terminal ends of the calcineurin A subunit (Figures 1D and S1U). We confirmed that the FRET ratio of a CFP-YFP version of the calcineurin probe is augmented upon Ca^{2+}/CaM addition. In keeping with previous structural pharmacological evidence, this FRET change was specifically inhibited by the calmodulin inhibitor W-7 (Figure S1V), but not by the calcineurin inhibitor FK506 complexed with FKBP that acts by hindering the substrate approach to the active site (Figure S1W) (Griffith et al., 1995; Kissinger et al., 1995). Thus, RY-CaN could accurately report the phosphatase activity that was induced by a conformational change triggered by binding to Ca^{2+}/CaM.

Single-Spine dFOMA Imaging of CaMKIIα and Calcineurin

Next, we compared the activation patterns of CaMKIIα and calcineurin induced by 20Hz-GU and 5Hz-GU in dendritic spines. We found that the activation frequency tuning for the two probes were distinct (Figure 1E): calcineurin was readily activated by 5Hz-GU in the stimulated spine, but not in the neighboring shafts or spines, and it showed invariable activation levels and kinetics with both 20Hz-GU and 5Hz-GU; in contrast, CaMKIIα showed differential responses to the two stimulation protocols, such that only 20Hz-GU triggered marked CaMKIIα activation. We also estimated the extent of CaMKIIα translocation into the stimulated spines, which had been shown to be associated with spine enlargement (Lee et al., 2009). Again, only 20Hz-GU triggered a significant increase in spine K2α fluorescence in the stimulated spines (Figure S1X), suggesting that the activation pattern of CaMKIIα, rather than that of calcineurin, is the major determinant of spine expansion in response to these stimulation protocols. Although activation kinetics of both RS-K2α and RY-CaN were similar and short-lived (returning to baseline in <1 min), in either 5Hz-GU or 20Hz-GU protocols (Figure 1E), we observed a distinct spatial pattern of the enzymatic activation against 20Hz-GU. CaMKIIα activation was mostly restricted in the stimulated spine, though we occasionally observed activation in the adjacent shaft in some limited cases. In contrast, calcineurin in the adjacent shaft was strongly activated to a level comparable to the stimulated spine (Figure 1E). Altogether, these results showed that individual dendritic spines are able to transform incoming glutamatergic

Cell PRESS
Open ACCESS

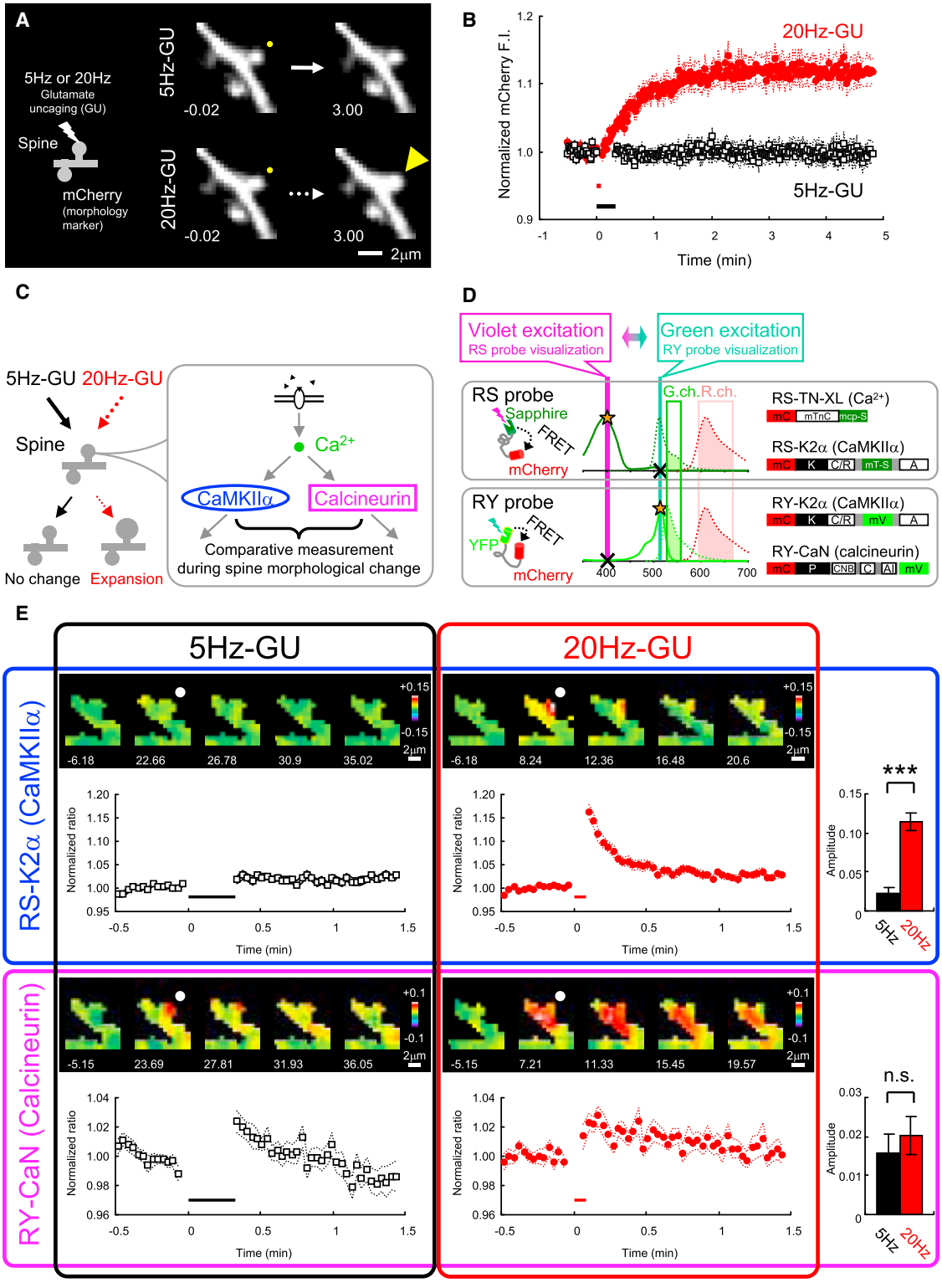

Figure 1. Investigation of Biochemical Correlates of Single-Spine Morphological Plasticity by dFOMA Imaging of CaMKIIα and Calcineurin

(A) Representative images of a spine and a hippocampal neuron before (–0.02 min) and after (3.00 min) 5Hz-GU or 20Hz-GU. The stimulated spine is indicated by yellow dots, and spine enlargement is indicated by a yellow arrowhead.

(B) The time course of normalized mCherry fluorescence intensity (F.I.) in spines subjected to 5Hz-GU and 20Hz-GU. Horizontal bars indicate periods of photostimulation. Data are mean (circles or squares) ± SEM (dashed lines) for 37 spines.

(legend continued on next page)

input sequences into distinct spatiotemporal activation patterns of CaMKIIα and calcineurin that were correlated with spine morphological changes.

Lack of Local Cross-regulation between CaMKIIα and Calcineurin during Activity-Regulated Spine Information Processing

Whereas calcineurin was activated by 5Hz-GU, both CaMKIIα and calcineurn were stimulated by 20Hz-GU. This raises the question of whether there is any cross-regulation between the two enzymes to tune the distinct response patterns. Indeed, several models had suggested a possible inhibition of CaMKIIα by calcineurin through the inhibitor-1-protein-phosphatase-1 pathway (Lisman 1989), so it was conceivable that calcineurin activated by 5Hz-GU could act to inhibit CaMKIIα to shift the kinase activation tuning toward 20Hz-GU. To directly address this issue, spines of neurons expressing K2α were stimulated by either 5Hz-GU or 20Hz-GU in the presence or absence of FK506. No significant effect of FK506 was observed on photostimulation-induced activation of CaMKIIα in dendritic spines (Figures 2A and 2B). A similar lack of FK506 effect was confirmed in dFOMA measurements in the neuronal soma stimulated at variable photostimulation frequencies; the addition of FK506 had little effect on the frequency-response curves of either RY-K2α or RS-TN-XL, a color variant of the troponin C-based Ca^{2+} indicator TN-XL (Mank et al., 2006) whose signal amplitude and kinetics were well correlated with those for Fluo-4FF, a low-affinity synthetic Ca^{2+} indicator often used for Ca^{2+} quantification (Figures S2A–S2D) (Yasuda et al., 2004). Although FK506 had no effect on RY-CaN FRET per se because of its specific action on the substrate interaction (Figures S1W and S2E), the inhibitory potency of FK506 that we used was confirmed in vitro (Figure S2F).

Interestingly, during FK506 pretreatment, we observed a slight but significant increase in baseline CaMKIIα activity prior to stimulation that was consistent with the idea that baseline calcineurin may regulate the baseline CaMKIIα activation state (Figures 2A and 2B, right panels, Figure S2G). Thus, although the calcineurin inhibitor might modulate pre-existing baseline activity of CaMKIIα, input-dependent CaMKIIα activation may be independent from any regulation by calcineurin. In keeping with this hypothesis, we found that the activation of CaMKIIα in spines was uncorrelated with that of calcineurin after either 20Hz-GU or 5Hz-GU (Figure 2C).

Altogether, these results clearly demonstrated that synapatically stimulated calcineurin activity had little impact on CaMKIIα activation induced by glutamate input and suggested that the crosstalk, if any, might be restricted to a rather mild, tonic regulation of the baseline activity level of CaMKIIα.

Deciphering the Coding Rules Underlying Glutamate Stimulation of CaMKIIα and Calcineurin

Having demonstrated the lack of local signal crosstalk during activity-dependent spine enlargement, we sought to decipher the biochemical rules that underlie input-specific and frequency-dependent information processing. To this end, we systematically varied the frequency and pulse number of photostimulation and determined the input-output functions or response surfaces of Ca^{2+}, CaMKIIα, and calcineurin (Figure 3A). To maximize the signal-to-noise ratio in our recordings, we performed high-speed dFOMA recording of Ca^{2+}-signaling components in the soma.

First, we quantified RS-K2α and RY-CaN responses in the same cell subjected to a 6 (frequency; 0.5, 1, 2, 5, 10, and 20 Hz) × 3 (number; 10, 20, and 30) matrix of photostimulation conditions (Figures 3B and S3A). At low photostimulation frequencies (~0.5 to 1 Hz), RY-CaN showed a moderate response, whereas RS-K2α showed no response (Figure 3B). Plotting of input-output response curves further revealed distinct information-processing features of CaMKIIα and calcineurin (Figures S3B and S3C). Thus, the amplitude and integral of the RS-K2α response were most sensitive to higher photostimulation frequencies (5 to 20 Hz) (Figures 3B and S3B). In contrast, whereas RY-CaN amplitude was somewhat more sensitive to a lower frequency range (~0.5 to 2 Hz), the RY-CaN integral remained insensitive to photostimulation frequency (Figures 3B and S3C). Altogether, and in spite of their comparable activation and decay kinetics (e.g., see the overlap of blue and pink traces at 20 Hz, 30 photostimulations in Figure 3B; Movie S1; Figure S3A), these results collectively suggested that the input-output properties of CaMKIIα and calcineurin were asymmetric and were governed by independent activation processes, in keeping with the findings obtained through spine dFOMA imaging (Figure 1).

Distinct Parameters of Ca^{2+} Dynamics Underlie Nonlinear Information Processing Mediated by CaMKIIα and Calcineurin

To examine how Ca^{2+} signal transduction processes affect the properties of the enzymatic output responses, we directly compared response kinetics and response surfaces for Ca^{2+} and CaMKIIα as well as for Ca^{2+} and calcineurin. Through

(C) An experimental design to test whether CaMKIIα and calcineurin can discriminate information of glutamate stimulation frequency.

(D) An optical recording strategy for dFOMA imaging. Excitation and emission spectra for Sapphire and mCherry as well as those for YFP and mCherry are shown (the excitation spectra of mCherry are omitted for clarity). The domain structures of the FRET probes are also shown. G.ch., green channel; R.ch., red channel; mC, mCherry; mTnC, mutant troponin C; mcp-S, monomeric and circularly permutated Sapphire; K, kinase domain; C/R, CaM binding/regulatory domain; mT-S, monomeric Turbo-Sapphire; A, association domain; mV, monomeric Venus; P, phosphatase domain; CNB, calcineurin B binding domain; C, CaM binding domain; and AI, autoinhibitory domain.

(E) CaMKIIα and calcineurin response to 5Hz-GU and 20Hz-GU. For each panel in the 2 × 2 matrix, representative time-lapsed $\Delta R/R_0$ images and mean response curves of RS-K2α (in the blue square) and RY-CaN (in the pink square) obtained in response to 5Hz-GU (in the black square) and 20Hz-GU (in the red square) are shown. In the representative images, the stimulated spines are indicated by white dots, and the time after stimulation onset is indicated in seconds. Right, the amplitude of RS-K2α (in the blue square) and RY-CaN (in the pink square) in stimulated spines in response to 5Hz-GU (black bar) or 20Hz-GU (red bar) are shown. Data are mean ± SEM for 28 spines. ***, $p < 0.001$; n.s, not significant (paired t test).

See also Figure S1.

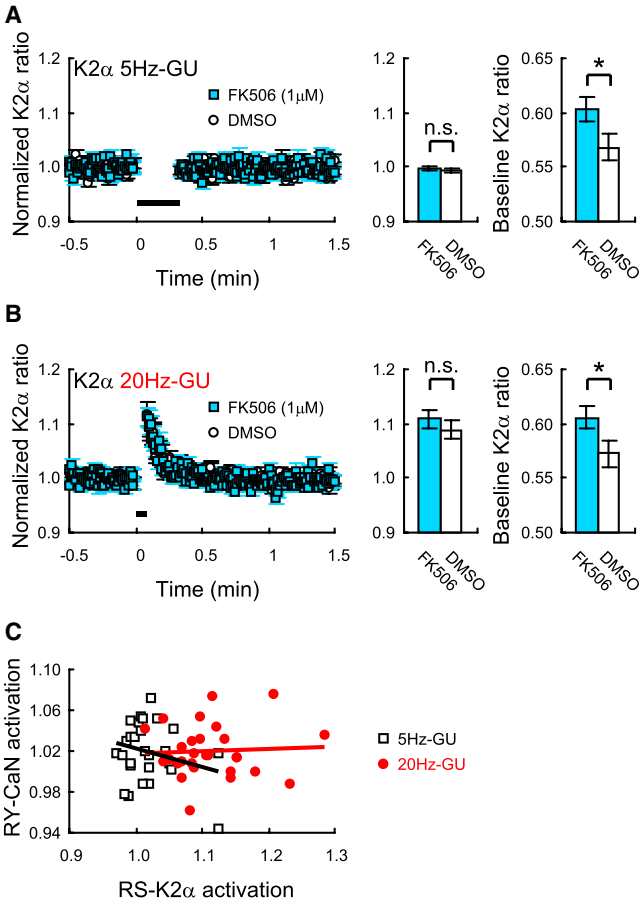

Figure 2. The Calcineurin Inhibitor FK506 has No Effect on Input-Stimulated CaMKIIα Activation but Mildly Augments Baseline CaMKIIα Activity

(A and B) Comparisons of dendritic spine K2α responses time course (left), amplitude (middle), and baseline CFP/YFP ratio (right) between in vehicle (0.05% DMSO, black open circle or black open bar, n = 42 spines, 14 neurons) and in 1 μM FK506 (sky blue square or sky blue bar, n = 42 spines, 14 neurons) against 5Hz-GU (A) and 20Hz-GU (B). Data are mean ± SEM. *, $p < 0.05$; n.s, not significant (paired t test).

(C) A population plot of RS-K2α and RY-CaN activation in stimulated spines in response to 5Hz-GU (black open squares) or 20Hz-GU (closed red circles). Each plot point represents an individual spine, and lines indicate the linear fit for 5Hz-GU responses (black line, $R^2 = 0.0614$) and 20Hz-GU responses (red line, $R^2 = 0.0022$).

See also Figure S2.

dFOMA imaging, activation of RY-K2α showed prolonged kinetics in comparison to activation of RS-TN-XL (Figures S4A and S4B; Movie S2), and, as expected, this sustained activation was dependent on the autophosphorylation of Thr286 and K2α (Figure S4C). We confirmed that all kinetics data were unaffected even by ~10-fold difference in probe expression levels (Figure S4D).

Next, the response surfaces for RS-TN-XL and RY-K2α were determined upon systematic interrogation under various conditions (frequency and number) of photostimulation (Figure 4A). Under all conditions, the amplitude of the RS-TN-XL response increased as either the frequency or pulse number of photostimulation increased (Figure 4B). In contrast, little or no RY-K2α response was observed under low-frequency (<5 Hz) or low-number (<10 pulses) photostimulation conditions (Figure 4C). However, frequency-dependent RY-K2α responses became evident when neurons were subjected to higher frequencies and higher pulse numbers of photostimulation (Figure 4C). Thus, a marked dual supralinear decoding of input frequency and number appeared to operate through CaMKIIα activation.

To calculate the degree of signal summation in the Ca^{2+}-CaMKIIα pathway, we experimentally measured RY-K2α FRET responses obtained at photostimulation pulse numbers of 20 or 30, compared these results with simulated responses obtained assuming a linear summation of FRET traces obtained at 10 pulses of photostimulation, and generated a nonlinearity index map (Figures 4D and 4E; see Extended Experimental Procedures). We found that the nonlinearity index for CaMKIIα mostly exceeded 2 at frequencies >5 Hz (Figure 4E). The index was closer to 1 for RS-TN-XL responses at all frequencies (Figures S4E and S4F). These results showed that two distinct rules of signal integration operate at different hierarchical levels; namely, a near-linear summation at the level of the second messenger Ca^{2+} and a supralinear summation during the activation of the downstream effector CaMKIIα.

After confirming that RS-TN-XL and RY-CaN also showed distinct activation kinetics and that their kinetics were unaffected by the expression levels of the probes expression levels of the probes (Figures S5A–S5C; Movie S3), we performed similar dFOMA imaging of these two components at various input frequencies and numbers (Figure 5A). The responses of RS-TN-XL in the presence of RY-CaN (Figure 5B) were basically identical to those in the presence of RY-K2α (Figure 4B). However, in contrast, RY-CaN showed marked responses at both low and high frequencies and pulse numbers of photostimulation (Figure 5C), indicating that the activation of calcineurin is achieved under much broader experimental conditions than in the case of CaMKIIα. The nonlinear index map of RY-CaN responses revealed a sublinearity that was especially pronounced at higher input frequencies and numbers (Figures 5D and 5E). The summation process of Ca^{2+} response in the same cells was mostly linear in the frequency-number range we examined. (Figures S5D and S5E). Thus, whereas the summation of calcineurin responses was linear at a low-input frequency, it became sublinear when inputs were delivered at a higher frequency and number. Altogether, we uncovered a characteristic role for calcineurin as an input number counter that was relatively immune to input frequency.

How could identical rises in Ca^{2+} result in such asymmetric activation profiles of downstream Ca^{2+}/CaM effectors? To address this, we assessed the contribution of either the amplitudes or integrals of activity-induced Ca^{2+} rises in achieving CaMKIIα or calcineurin activation (Figure 5F). Whereas the information about both glutamate input number and frequency were linearly encoded into amplitudes of intracellular Ca^{2+} rises, the frequency information had little influence in determining the Ca^{2+} integral (Figure 5F). The amplitudes, as well as the integrals, of either CaMKIIα or calcineurin activation were most correlated with profiles of either Ca^{2+} amplitudes or Ca^{2+} integrals, respectively (Figure 5F). As a consequence, CaMKIIα, which effectively

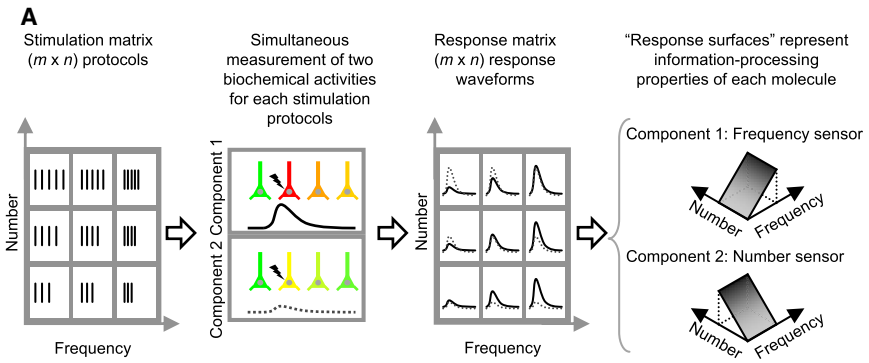

Figure 3. The Number and Frequency of Neuronal Inputs Independently Control the Activities of CaMKIIα and Calcineurin in Hippocampal Neurons

(A) An experimental workflow for the examination of biochemical information processing in neurons. (B) A response matrix for RS-K2α and RY-CaN corresponding to a 6 × 3 photostimulation matrix. Each trace represents an averaged dual FRET recording obtained from the soma of cultured hippocampal neurons with the various stimulation regimens (n = 6 neurons).

See also Figure S3.

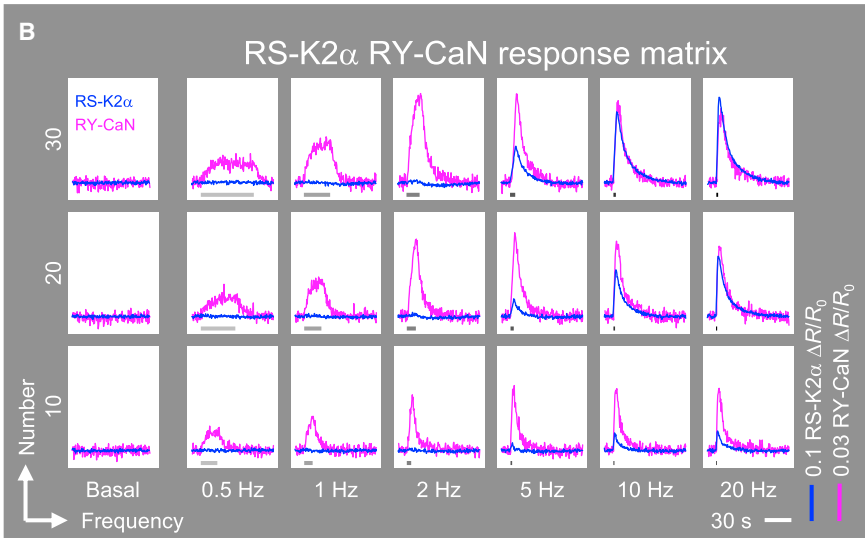

read out Ca^{2+} amplitude information, was most effective for activation under conditions when both the frequency and pulse number are relatively high. This property allowed CaMKIIα to function as an input frequency/number decoder. In contrast, calcineurin showed little dependence on input frequency, allowing it to function as an input number counter. Thus, the resulting bandwidth separation may stem from the unique distinction of Ca^{2+} information that CaMKIIα (Figure 5F, bottom left) and calcineurin (Figure 5F, bottom right) read out in hippocampal neurons. Altogether, these lines of evidence indicated that CaMKIIα and calcineurin are unique molecular "switches" dedicated to decoding distinct, yet complementary, parameters of activity-induced intracellular Ca^{2+} rises, amplitude and integral, respectively.

DISCUSSION

Asymmetric and Distinctive Information Processing by CaMKIIα and Calcineurin Allow Efficient Information Extraction from Neuronal Input Sequences

We have developed an optical platform, dFOMA imaging, and examined how information about neuronal input parameters is processed and represented in the biochemical activities of CaMKIIα and calcineurin in the neuronal soma and dendritic spines.

The tuning properties of CaMKIIα and calcineurin might be accounted for, in part, by some of the characteristic biochemical properties of these two enzymes, including CaM binding and autophosphorylation (Meyer et al., 1992; Deisseroth et al., 1995; De Koninck and Schulman, 1998; Bradshaw et al., 2003) as well as the calcineurin's relatively high affinity for Ca^{2+} and its time- and Ca^{2+}-CaM-dependent inactivation (Stemmer and Klee, 1994; Gaertner et al., 2004; Quintana et al., 2005). However, the asymmetric and distinctive nature of the newly uncovered input-tuning property of these enzymes was entirely unpredicted. Further detailed kinetic studies will be required to tease apart the unitary processes underlying these basic properties and to better understand the dynamic nonlinear processing of Ca^{2+} signal effectors.

Temporally Overlapping but Spatially Distinct Activation Domains of CaMKIIα and Calcineurin during Spine Morphological Plasticity

In accord with the frequency and number decoder function of CaMKIIα, we found that 5Hz-GU efficiently activated calcineurin, but not CaMKIIα, in the dendritic spines. However, until now, it has remained unclear whether 20Hz-GU activates both of the enzymes or only CaMKIIα. Our dFOMA recording showed that both CaMKIIα and calcineurin activities were stimulated immediately.

Temporally, both enzyme activities decayed rapidly after cessation of the stimulus in a highly graded manner. Even under conditions where spine morphological expansion was stably induced by 20Hz-GU, deactivation of CaMKIIα to the baseline level occurred within ~30 s to 1 min, consistent with previous observations (Lengyel et al., 2004; Lee et al., 2009; Buard et al., 2010; Coultrap and Bayer, 2012; see also Barria et al., 1997). Although our data on both CaMKIIα and calcineurin are in sharp contrast to prevailing views of metastable activation of plasticity-inducing enzymes, the possibility exists that some forms of metastability may be expressed in nanodomains, perhaps in

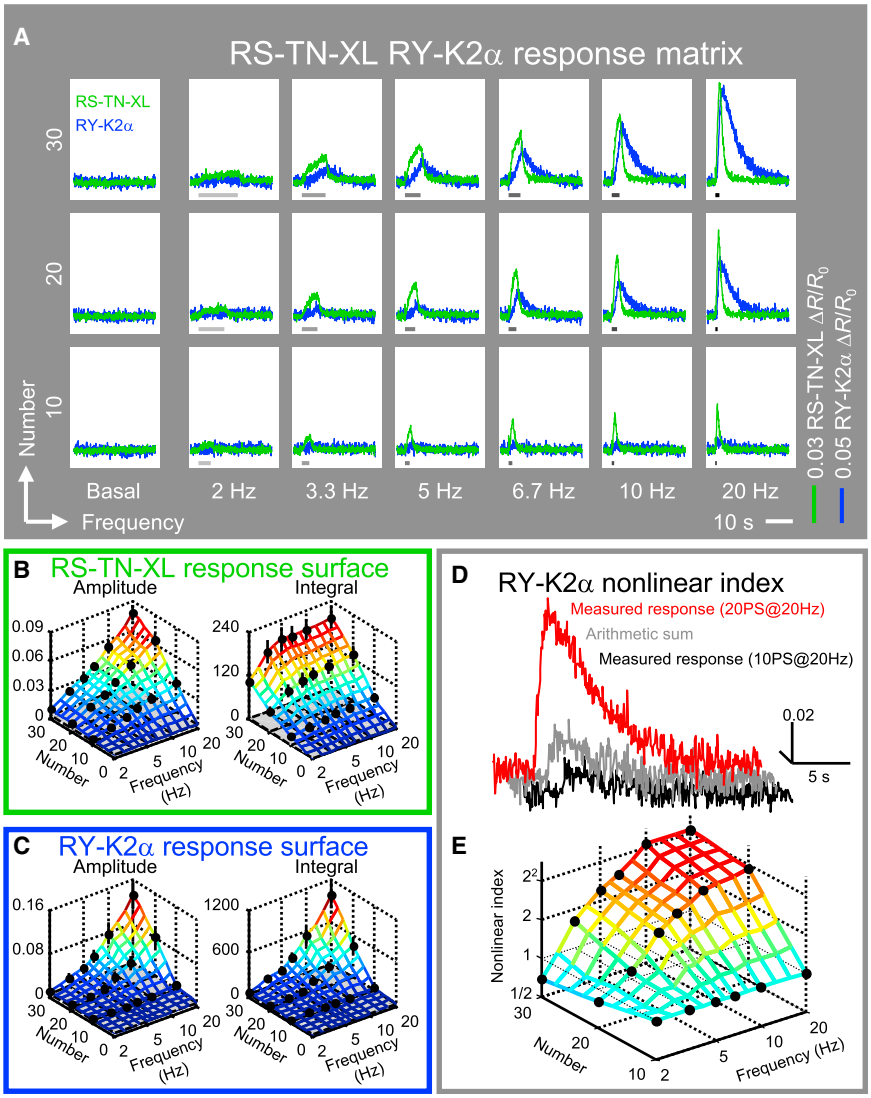

Figure 4. CaMKIIα Functions as a Decoder for Both High-Frequency and High-Number-of-Input Events via Supralinear Signal Integration

(A) A response matrix for RS-TN-XL and RY-K2α obtained with a 6 × 3 photostimulation matrix. Each trace represents an averaged dual FRET signal obtained from the soma of cultured hippocampal neurons with multiple randomized stimulation regimens (n = 12 neurons).

(B and C) Response surfaces for the amplitude and integral of RS-TN-XL (B) and RY-K2α (C) signals. Black circles and bars indicate mean ± SEM for each stimulation parameter (n = 12 neurons).

(D) A comparison of an experimentally determined averaged response for RY-K2α obtained with 20 photostimulations (PS) at a frequency of 20 Hz (red) with a simulated linear arithmetic sum (gray) that is based on an averaged response trace obtained with 10 photostimulations at 20 Hz (black).

(E) A nonlinear index map for RY-K2α plotted against photostimulation frequency and pulse number.

See also Figure S4.

association with specific postsynaptic density scaffolds, given that a minor fraction of CaMKIIα has been suggested to bind to NMDA receptors and retain autonomous activity (Bayer et al., 2001; Feng et al., 2011).

Spatially, however, we found that the activation domains of CaMKIIα and calcineurin were clearly separated. If CaMKIIα and calcineurin were interfering with each other during spine plasticity, the larger spatial spread of calcineurin during high-frequency stimulation might dominate and constrain CaMKIIα-mediated spine morphological plasticity. However, this was unlikely for three reasons. First, our measurements showed that spine CaMKIIα activity was uncorrelated from spine CaN activity during maximal activity (Figure 2C). Second, inhibition of calcineurin with FK506 had no effect on input-stimulated CaMKIIα activity (Figures 2A and 2B). Third, previous reports showed a minimal effect on long-term potentiation induction in various calcineurin and inhibitor-1 knockout mouse lines (Zhuo et al., 1999; Allen et al., 2000; Zeng et al., 2001). In keeping with this independence, CaMKIIα and calcineurin were shown to distinctively associate with either a GluN2B complex or an AKAP150 complex in the spines. Altogether, these results indicated that CaMKIIα and calcineurin might independently process neuronal input patterns.

Combinatorial Representation of Neuronal Input Information on a Ca^{2+}-CaMKIIα-Calcineurin Activity Space May Provide a Substrate for Determining Input-Dependent Plasticity

We found that that spines executed structural plasticity in a frequency-dependent manner on the basis of CaMKIIα's activation-frequency-tuning properties, in keeping with the previous results that CaMKII is involved in the morphological changes of spines (Matsuzaki et al., 2004; Lee et al., 2009). In contrast, we were unable to find spine morphological alteration that was specifically associated with the frequency dependence of calcineurin activation. However, given that calcineurin activation was observed during chemical induction of long-term depression (H.F. and H.B., unpublished data), calcineurin might potentially be involved in other forms of functional remodeling of synapses.

If we assume that information about neuronal input parameters can be decoded as the relative ratio of these enzyme activities and that the activation of CaMKIIα and of calcineurin proceed independently but should be functionally coordinated to optimize the separability of the activation threshold, our measured data can be readily accommodated into a unified input-response surface that is reminiscent of a Bienenstock-Cooper-Munro (BCM)-type plasticity implementation curve (Bienenstock et al., 1982) (Figure 5G). In our model, a BCM-like

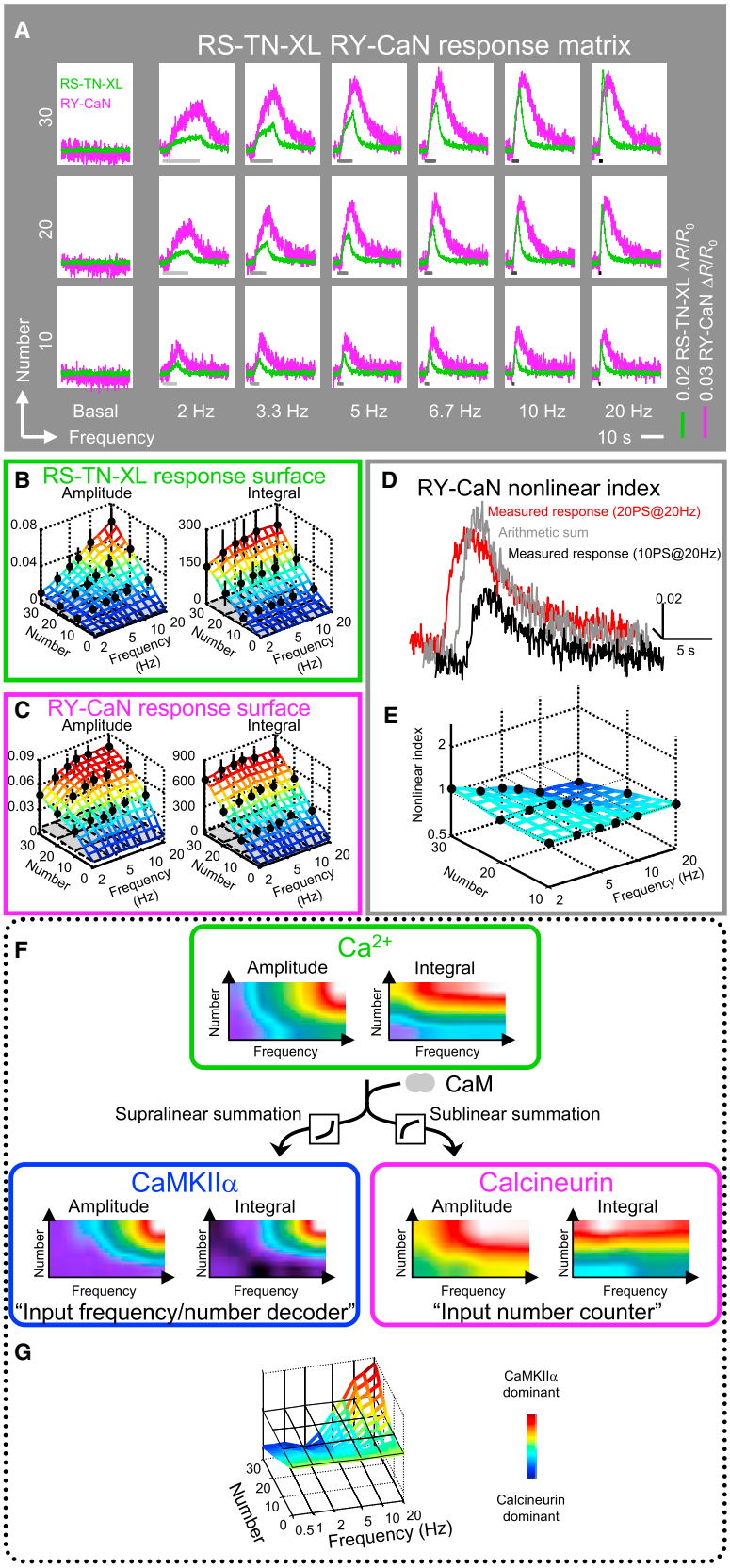

Figure 5. Calcineurin Functions as an Input Number Counter Tuned to Lower-Input Frequencies and Numbers and Implements Biochemical Information Processing of Low-Frequency Events via Sublinear Signal Integration

(A) A response matrix for RS-TN-XL and RY-CaN obtained with a 6 × 3 photostimulation matrix. Each trace represents an averaged dual FRET signal obtained from the soma of cultured hippocampal neurons with multiple randomized stimulation regimens (n = 9 neurons).

(B and C) Response surfaces for the amplitude and integral of RS-TN-XL (B) and RY-CaN (C) signals. Black circles and bars indicate mean ± SEM for each stimulation parameter (n = 9 neurons).

(D) A comparison of an experimentally determined averaged response for RY-CaN obtained with 20 photostimulations (PS) at 20 Hz (red) to a simulated linear arithmetic sum (gray) that is based on an averaged response trace obtained with 10 photostimulations at 20 Hz (black).

(E) A nonlinear index map for RY-CaN plotted against photostimulation frequency and number.

(F) An integrative model of biochemical Ca^{2+} signal summation based on dFOMA data; color-coded isoactivity maps for Ca^{2+} (top panels), CaMKIIα (bottom left), and calcineurin (bottom right) are shown as a function of glutamatergic input number and frequency (real data obtained from amplitude and integrals of FRET ratio transients were interpolated).

(G) A three-dimensional representation of combinatorial Ca^{2+} signal processing operated by CaMKIIα and calcineurin. We generally assume that CaMKIIα and calcineurin activities mediate distinct cellular outcomes in neurons; however, for clarity, we represent them in opposite polarity on the same z axis as functions of input number (y axis) and frequency (x axis). A relative map of summated CaMKIIα and calcineurin activities was drawn only on the basis of the assumption that the integrals of the two enzyme activities are balanced at 20 photostimulations at 10 Hz. An oblique three-dimensional rendering reveals that a BCM-like curve becomes apparent in the x-z plane at an input number of 30.

See also Figure S5.

curve only appears with higher-input numbers ($\geq$30). Consistent with this prediction, studies of spike-timing-dependent plasticity revealed that repeated short-interval stimulus pairs (in the order of 20 to 60) were necessary to induce potentiation or depression (Bi and Poo, 1998). Further application of dFOMA studies will undoubtedly help clarify the biochemical basis of neuronal computation achieved by the synaptic network of signaling pathways.

EXPERIMENTAL PROCEDURES

Cell Culture and Neuronal Stimulation

Cultures of rat dissociated hippocampal neurons were prepared for imaging as described previously (Furuyashiki et al., 2002) with minor modifications. At 10 to 13 days in vitro, the neurons were transfected by lipofection with plasmids encoding RS-K2α and RY-CaN, RS-TN-XL and RY-K2α, RS-TN-XL and RY-CaN, or mCherry and K2α. After 1 to 3 days, the neurons were subjected to dFOMA imaging in Mg^{2+}-free Tyrode's solution (129 mM NaCl, 5 mM KCl, 30 mM glucose, 25 mM HEPES-NaOH [pH 7.4], and 2 mM $CaCl_2$; osmolality was adjusted to that of the conditioned culture medium [~330 milliosmoles/kg]) supplemented with 0.5 mM MNI-glutamate (Tocris Bioscience) and 1 μM tetrodotoxin to prevent contamination from spontaneous and recurrent activity. Detailed methods for dFOMA imaging and a pharmacological assessment of K2α activation are described in the Extended Experimental Procedures. All animal experiments in this study were performed in accordance with regulations and guidelines for the care and use of experimental animals of the University of Tokyo and approved by the institutional review committee of University of Tokyo Graduate School of Medicine.

Quantitative Image Analysis

Acquired time-lapse images were processed and analyzed offline with AQUACOSMOS (Hamamatsu Photonics), Metamorph (Molecular Devices), Image J, MATLAB (MathWorks), Origin (OriginLab), and Excel (Microsoft).

Additional experimental details can be found in the Extended Experimental Procedures.

SUPPLEMENTAL INFORMATION

Supplemental Information includes Extended Experimental Procedures, five figures, and three movies and can be found with this article online at http://dx.doi.org/10.1016/j.celrep.2013.03.033.

LICENSING INFORMATION

ACKNOWLEDGMENTS

We thank all members of the Bito laboratory for discussion; O. Griesbeck for T-Sapphire, cpT-Sapphire 174–173, and TN-XL complementary DNAs (cDNAs); A. Miyawaki for Venus cDNA; R.Y. Tsien for mCherry cDNA; T. Furukawa, H. Nidaira (Olympus), H. Sugiyama, K. Suzuki, and Y. Tsuchiya (Hamamatsu Photonics) for advice on the imaging system; K Hanaoka, K. Kikuchi, T. Komatsu, T. Nagai, and T. Nagano for advice on FRET; S. Nakanishi, K. Moriyoshi, K. Miki, and D. Watanabe for encouragement; K. Saiki, Y. Kondo, R. Gyobu, and T. Kinbara for assistance. This work was supported in part by Grants-in-Aid for Scientific Research from the Ministry of Education, Culture, Sports, Science & Technology in Japan (innovative areas Comprehensive Brain Science Network and Fluorescence Live Imaging to H.B.), from the Japan Society for the Promotion of Science (KIBAN to H.O.; WAKATE to S.T.-K. and H.B.), from the Japanese Ministry of Health, Labour and Welfare (to H.O. and H.B.), from a Global COE Program (to H.B.), and by awards from the Astellas Foundation for Research on Metabolic Disorders, the Kowa Life Science Foundation, the Shimadzu Science Foundation, the Takeda Foundation, the Toray Science Foundation, and the Yamada Science Foundation (to H.B.).

Received: February 19, 2013
Revised: March 18, 2013
Accepted: March 20, 2013
Published: April 18, 2013

REFERENCES

Allen, P.B., Hvalby, O., Jensen, V., Errington, M.L., Ramsay, M., Chaudhry, F.A., Bliss, T.V., Storm-Mathisen, J., Morris, R.G., Andersen, P., and Greengard, P. (2000). Protein phosphatase-1 regulation in the induction of long-term potentiation: heterogeneous molecular mechanisms. J. Neurosci. *20*, 3537–3543.

Barria, A., Muller, D., Derkach, V., Griffith, L.C., and Soderling, T.R. (1997). Regulatory phosphorylation of AMPA-type glutamate receptors by CaM-KII during long-term potentiation. Science *276*, 2042–2045.

Bayer, K.U., De Koninck, P., Leonard, A.S., Hell, J.W., and Schulman, H. (2001). Interaction with the NMDA receptor locks CaMKII in an active conformation. Nature *411*, 801–805.

Bhalla, U.S. (2002). Biochemical signaling networks decode temporal patterns of synaptic input. J. Comput. Neurosci. *13*, 49–62.

Bi, G.Q., and Poo, M.M. (1998). Synaptic modifications in cultured hippocampal neurons: dependence on spike timing, synaptic strength, and postsynaptic cell type. J. Neurosci. *18*, 10464–10472.

Bienenstock, E.L., Cooper, L.N., and Munro, P.W. (1982). Theory for the development of neuron selectivity: orientation specificity and binocular interaction in visual cortex. J. Neurosci. *2*, 32–48.

Bito, H. (1998). The role of calcium in activity-dependent neuronal gene regulation. Cell Calcium *23*, 143–150.

Bito, H., and Takemoto-Kimura, S. (2003). Ca^{2+}/CREB/CBP-dependent gene regulation: a shared mechanism critical in long-term synaptic plasticity and neuronal survival. Cell Calcium *34*, 425–430.

Bliss, T.V., and Collingridge, G.L. (1993). A synaptic model of memory: long-term potentiation in the hippocampus. Nature *361*, 31–39.

Bradshaw, J.M., Kubota, Y., Meyer, T., and Schulman, H. (2003). An ultrasensitive Ca^{2+}/calmodulin-dependent protein kinase II-protein phosphatase 1 switch facilitates specificity in postsynaptic calcium signaling. Proc. Natl. Acad. Sci. USA *100*, 10512–10517.

Branco, T., Clark, B.A., and Häusser, M. (2010). Dendritic discrimination of temporal input sequences in cortical neurons. Science *329*, 1671–1675.

Buard, I., Coultrap, S.J., Freund, R.K., Lee, Y.S., Dell'Acqua, M.L., Silva, A.J., and Bayer, K.U. (2010). CaMKII "autonomy" is required for initiating but not for maintaining neuronal long-term information storage. J. Neurosci. *30*, 8214–8220.

Chao, L.H., Stratton, M.M., Lee, I.H., Rosenberg, O.S., Levitz, J., Mandell, D.J., Kortemme, T., Groves, J.T., Schulman, H., and Kuriyan, J. (2011). A mechanism for tunable autoinhibition in the structure of a human Ca^{2+}/calmodulin- dependent kinase II holoenzyme. Cell *146*, 732–745.

Colbran, R.J. (2004). Protein phosphatases and calcium/calmodulin-dependent protein kinase II-dependent synaptic plasticity. J. Neurosci. *24*, 8404–8409.

Coultrap, S.J., and Bayer, K.U. (2012). CaMKII regulation in information processing and storage. Trends Neurosci. *35*, 607–618.

De Koninck, P., and Schulman, H. (1998). Sensitivity of CaM kinase II to the frequency of Ca^{2+} oscillations. Science *279*, 227–230.

Deisseroth, K., Bito, H., Schulman, H., and Tsien, R.W. (1995). Synaptic plasticity: A molecular mechanism for metaplasticity. Curr. Biol. *5*, 1334–1338.

Dudek, S.M., and Bear, M.F. (1992). Homosynaptic long-term depression in area CA1 of hippocampus and effects of N-methyl-D-aspartate receptor blockade. Proc. Natl. Acad. Sci. USA *89*, 4363–4367.

Feng, B., Raghavachari, S., and Lisman, J. (2011). Quantitative estimates of the cytoplasmic, PSD, and NMDAR-bound pools of CaMKII in dendritic spines. Brain Res. *1419*, 46–52.

Furuyashiki, T., Arakawa, Y., Takemoto-Kimura, S., Bito, H., and Narumiya, S. (2002). Multiple spatiotemporal modes of actin reorganization by NMDA receptors and voltage-gated Ca^{2+} channels. Proc. Natl. Acad. Sci. USA *99*, 14458–14463.

Gaertner, T.R., Kolodziej, S.J., Wang, D., Kobayashi, R., Koomen, J.M., Stoops, J.K., and Waxham, M.N. (2004). Comparative analyses of the three-dimensional structures and enzymatic properties of alpha, beta, gamma and delta isoforms of Ca^{2+}-calmodulin-dependent protein kinase II. J. Biol. Chem. *279*, 12484–12494.

Griffith, J.P., Kim, J.L., Kim, E.E., Sintchak, M.D., Thomson, J.A., Fitzgibbon, M.J., Fleming, M.A., Caron, P.R., Hsiao, K., and Navia, M.A. (1995). X-ray structure of calcineurin inhibited by the immunophilin-immunosuppressant FKBP12-FK506 complex. Cell *82*, 507–522.

Hudmon, A., and Schulman, H. (2002). Neuronal Ca^{2+}/calmodulin-dependent protein kinase II: the role of structure and autoregulation in cellular function. Annu. Rev. Biochem. *71*, 473–510.

Kissinger, C.R., Parge, H.E., Knighton, D.R., Lewis, C.T., Pelletier, L.A., Tempczyk, A., Kalish, V.J., Tucker, K.D., Showalter, R.E., Moomaw, E.W., et al. (1995). Crystal structures of human calcineurin and the human FKBP12-FK506-calcineurin complex. Nature *378*, 641–644.

Klee, C.B. (1991). Concerted regulation of protein phosphorylation and dephosphorylation by calmodulin. Neurochem. Res. *16*, 1059–1065.

Lee, S.J., Escobedo-Lozoya, Y., Szatmari, E.M., and Yasuda, R. (2009). Activation of CaMKII in single dendritic spines during long-term potentiation. Nature *458*, 299–304.

Lengyel, I., Voss, K., Cammarota, M., Bradshaw, K., Brent, V., Murphy, K.P., Giese, K.P., Rostas, J.A., and Bliss, T.V. (2004). Autonomous activity of CaMKII is only transiently increased following the induction of long-term potentiation in the rat hippocampus. Eur. J. Neurosci. *20*, 3063–3072.

Lisman, J. (1989). A mechanism for the Hebb and the anti-Hebb processes underlying learning and memory. Proc. Natl. Acad. Sci. USA *86*, 9574–9578.

Malenka, R.C., and Bear, M.F. (2004). LTP and LTD: an embarrassment of riches. Neuron *44*, 5–21.

Malinow, R., Madison, D.V., and Tsien, R.W. (1988). Persistent protein kinase activity underlying long-term potentiation. Nature *335*, 820–824.

Malleret, G., Haditsch, U., Genoux, D., Jones, M.W., Bliss, T.V., Vanhoose, A.M., Weitlauf, C., Kandel, E.R., Winder, D.G., and Mansuy, I.M. (2001). Inducible and reversible enhancement of learning, memory, and long-term potentiation by genetic inhibition of calcineurin. Cell *104*, 675–686.

Mank, M., Reiff, D.F., Heim, N., Friedrich, M.W., Borst, A., and Griesbeck, O. (2006). A FRET-based calcium biosensor with fast signal kinetics and high fluorescence change. Biophys. J. *90*, 1790–1796.

Matsuzaki, M., Honkura, N., Ellis-Davies, G.C., and Kasai, H. (2004). Structural basis of long-term potentiation in single dendritic spines. Nature *429*, 761–766.

Meyer, T., Hanson, P.I., Stryer, L., and Schulman, H. (1992). Calmodulin trapping by calcium-calmodulin-dependent protein kinase. Science *256*, 1199–1202.

Mulkey, R.M., Endo, S., Shenolikar, S., and Malenka, R.C. (1994). Involvement of a calcineurin/inhibitor-1 phosphatase cascade in hippocampal long-term depression. Nature *369*, 486–488.

Nagai, T., Ibata, K., Park, E.S., Kubota, M., Mikoshiba, K., and Miyawaki, A. (2002). A variant of yellow fluorescent protein with fast and efficient maturation for cell-biological applications. Nat. Biotechnol. *20*, 87–90.

Quintana, A.R., Wang, D., Forbes, J.E., and Waxham, M.N. (2005). Kinetics of calmodulin binding to calcineurin. Biochem. Biophys. Res. Commun. *334*, 674–680.

Shaner, N.C., Campbell, R.E., Steinbach, P.A., Giepmans, B.N., Palmer, A.E., and Tsien, R.Y. (2004). Improved monomeric red, orange and yellow fluorescent proteins derived from Discosoma sp. red fluorescent protein. Nat. Biotechnol. *22*, 1567–1572.

Silva, A.J., Stevens, C.F., Tonegawa, S., and Wang, Y. (1992). Deficient hippocampal long-term potentiation in alpha-calcium-calmodulin kinase II mutant mice. Science *257*, 201–206.

Stemmer, P.M., and Klee, C.B. (1994). Dual calcium ion regulation of calcineurin by calmodulin and calcineurin B. Biochemistry *33*, 6859–6866.

Sumi, M., Kiuchi, K., Ishikawa, T., Ishii, A., Hagiwara, M., Nagatsu, T., and Hidaka, H. (1991). The newly synthesized selective Ca^{2+}/calmodulin dependent protein kinase II inhibitor KN-93 reduces dopamine contents in PC12h cells. Biochem. Biophys. Res. Commun. *181*, 968–975.

Takao, K., Okamoto, K., Nakagawa, T., Neve, R.L., Nagai, T., Miyawaki, A., Hashikawa, T., Kobayashi, S., and Hayashi, Y. (2005). Visualization of synaptic Ca^{2+} /calmodulin-dependent protein kinase II activity in living neurons. J. Neurosci. *25*, 3107–3112.

Wyatt, R.M., Tring, E., and Trachtenberg, J.T. (2012). Pattern and not magnitude of neural activity determines dendritic spine stability in awake mice. Nat. Neurosci. *15*, 949–951.

Yasuda, R., Nimchinsky, E.A., Scheuss, V., Pologruto, T.A., Oertner, T.G., Sabatini, B.L., and Svoboda, K. (2004). Imaging calcium concentration dynamics in small neuronal compartments. Sci. STKE *2004*, pl5.

Zapata-Hommer, O., and Griesbeck, O. (2003). Efficiently folding and circularly permuted variants of the Sapphire mutant of GFP. BMC Biotechnol. *3*, 5.

Zeng, H., Chattarji, S., Barbarosie, M., Rondi-Reig, L., Philpot, B.D., Miyakawa, T., Bear, M.F., and Tonegawa, S. (2001). Forebrain-specific calcineurin knockout selectively impairs bidirectional synaptic plasticity and working/episodic-like memory. Cell *107*, 617–629.

Zhou, Q., Homma, K.J., and Poo, M.M. (2004). Shrinkage of dendritic spines associated with long-term depression of hippocampal synapses. Neuron *44*, 749–757.

Zhuo, M., Zhang, W., Son, H., Mansuy, I., Sobel, R.A., Seidman, J., and Kandel, E.R. (1999). A selective role of calcineurin aalpha in synaptic depotentiation in hippocampus. Proc. Natl. Acad. Sci. USA *96*, 4650–4655.